

Generation of nanobodies with conformational specificity for tau oligomers that recognize tau aggregates from human Alzheimer's disease samples

Nikki McArthur¹, Jay D. Squire¹, Ogechukwu J. Onyeachonam¹, Nemil N. Bhatt^{2,3}, Cynthia Jerez^{2,3}, Abigail L. Holberton⁴, Peter M. Tessier^{5,6,7,8}, Levi B. Wood^{4,9,10}, Rakez Kaye^{2,3}, Ravi S. Kane^{1,9,10*}

¹School of Chemical & Biomolecular Engineering, Georgia Institute of Technology, Atlanta, Georgia 30332, USA

²Mitchell Center for Neurodegenerative Disease, University of Texas Medical Branch, Galveston, Texas 77555, USA

³Department of Neurology, University of Texas Medical Branch, Galveston, Texas 77555, USA

⁴George W. Woodruff School of Mechanical Engineering, Georgia Institute of Technology, Atlanta, Georgia 30332, USA

⁵Department of Chemical Engineering, University of Michigan, North Campus Research Complex, 2800 Plymouth Road, Ann Arbor, MI 48109, USA

⁶Biointerfaces Institute, University of Michigan, Ann Arbor, MI 48109, USA

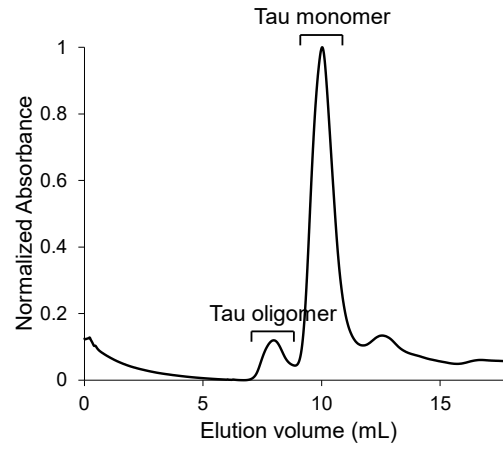
⁷Department of Pharmaceutical Sciences, University of Michigan, Ann Arbor, MI 48109, USA

⁸Department of Biomedical Engineering, University of Michigan, Ann Arbor, MI 48109, USA

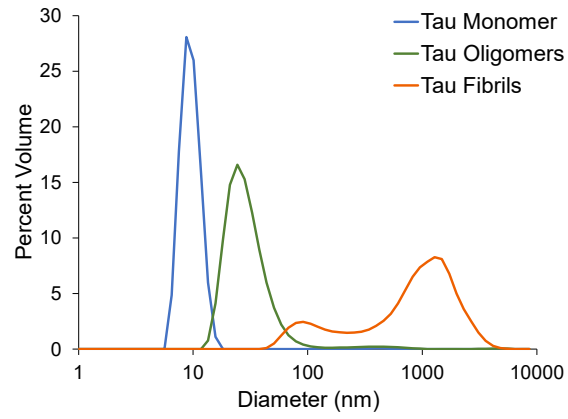
⁹Wallace H. Coulter Department of Biomedical Engineering, Georgia Institute of Technology, Atlanta, Georgia 30332, USA

¹⁰Parker H. Petit Institute for Bioengineering and Bioscience, Georgia Institute of Technology, Atlanta, Georgia 30332, USA

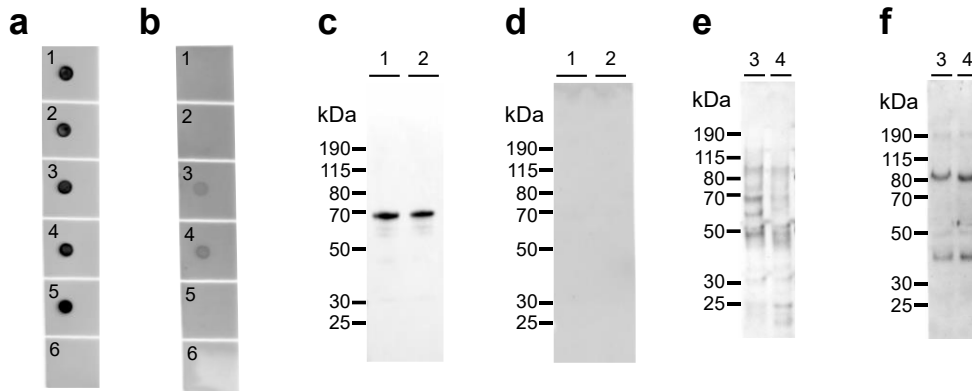
* To whom correspondence should be addressed: ravi.kane@chbe.gatech.edu



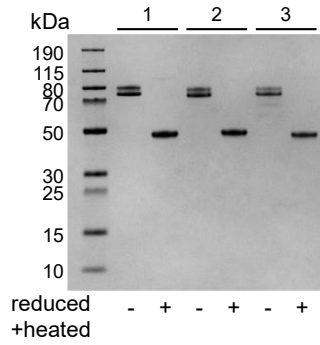
Supplementary Figure 1. Size exclusion chromatography trace for the separation of tau monomer and oligomers.



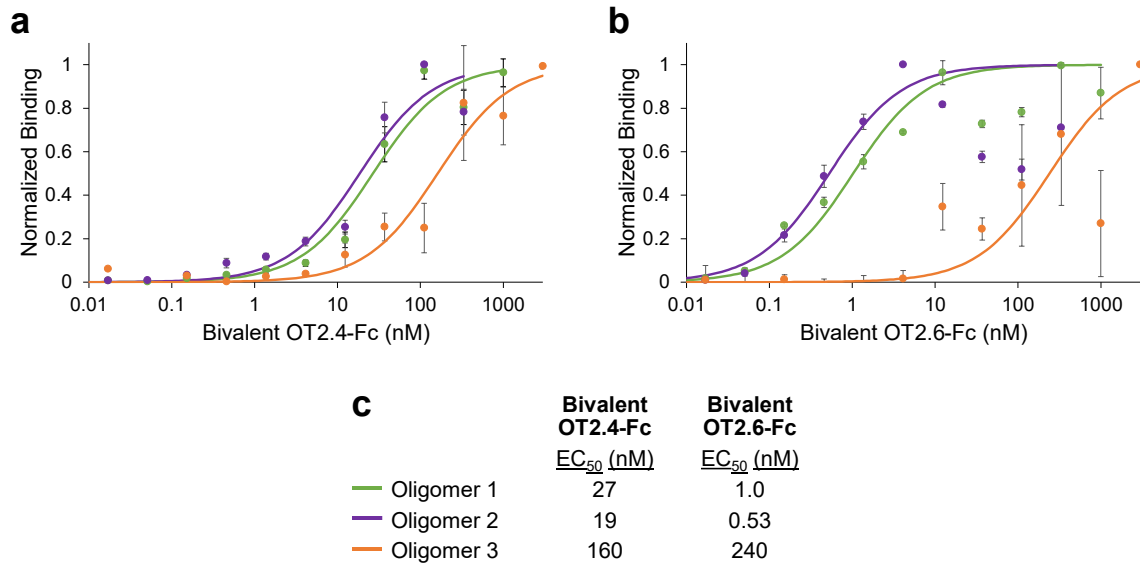
Supplementary Figure 2. Characterization of tau monomer (blue), oligomers (green), and fibrils (orange) by dynamic light scattering.



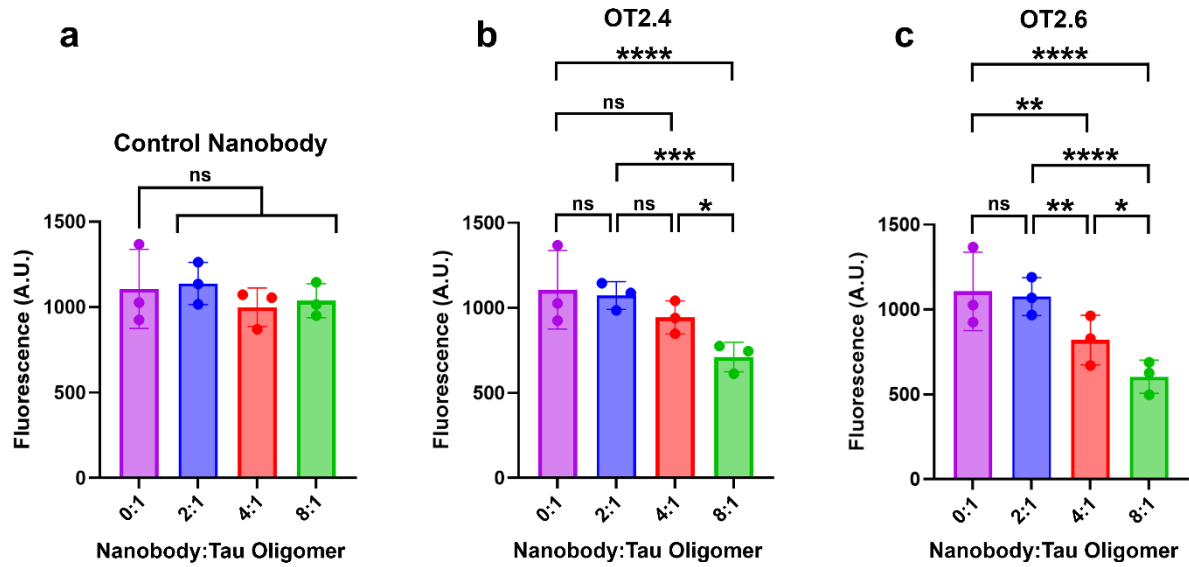
Supplementary Figure 3. (a-b) Characterization of (1) tau monomer, (2) biotinylated tau monomer, (3) tau oligomers, (4) biotinylated tau oligomers, (5) tau fibrils, and (6) BSA by dot blot with (a) Tau5 antibody and (b) T22 antibody. Unprocessed images of these membranes are shown in **Supplementary Figure 9c and d**. (c-f) Characterization of (1) tau monomer, (2) biotinylated tau monomer, (3) tau oligomers, and (4) biotinylated tau oligomers by western blot with (c, e) Tau5 antibody and (d, f) T22 antibody. Ponceau S staining of these membranes is shown in **Supplementary Figure 8e and f**, and unprocessed images of these membranes are shown in **Supplementary Figure 9e-h**.



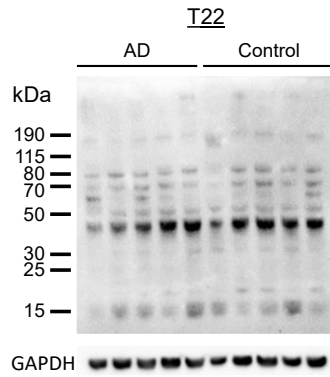
Supplementary Figure 4. An SDS-PAGE gel containing (1) bivalent OT2.4-Fc, (2) bivalent OT2.6-Fc, and (3) bivalent MT3.1-Fc. Reduced and heated samples are indicated with “+” and samples that are not reduced or heated are indicated with “-”. An unprocessed image of this gel is shown in **Supplementary Figure 9i**.



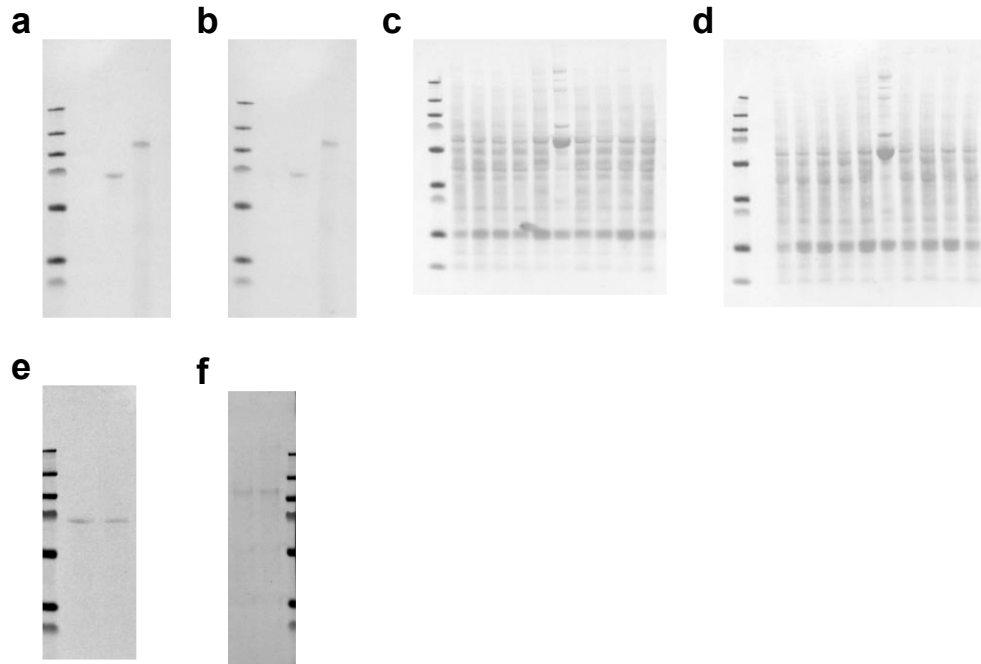
Supplementary Figure 5. a-b) Binding of **(a)** bivalent OT2.4-Fc or **(b)** bivalent OT2.6-Fc to tau oligomer samples 1 and 2 (separate preparations produced using the protocol described in the methods section) and sample 3 (prepared using a different method as previously described^{1,2}) was assessed with dot blots, quantified, and plotted as a function of Fc fusion construct concentration. Data points are averages from three repeats and error bars indicate standard deviation. **c)** EC_{50} s for the binding of the Fc fusion constructs to tau oligomer samples were calculated using a global nonlinear least-squares fit of the data presented in **Supplementary Figure 5a and b**.



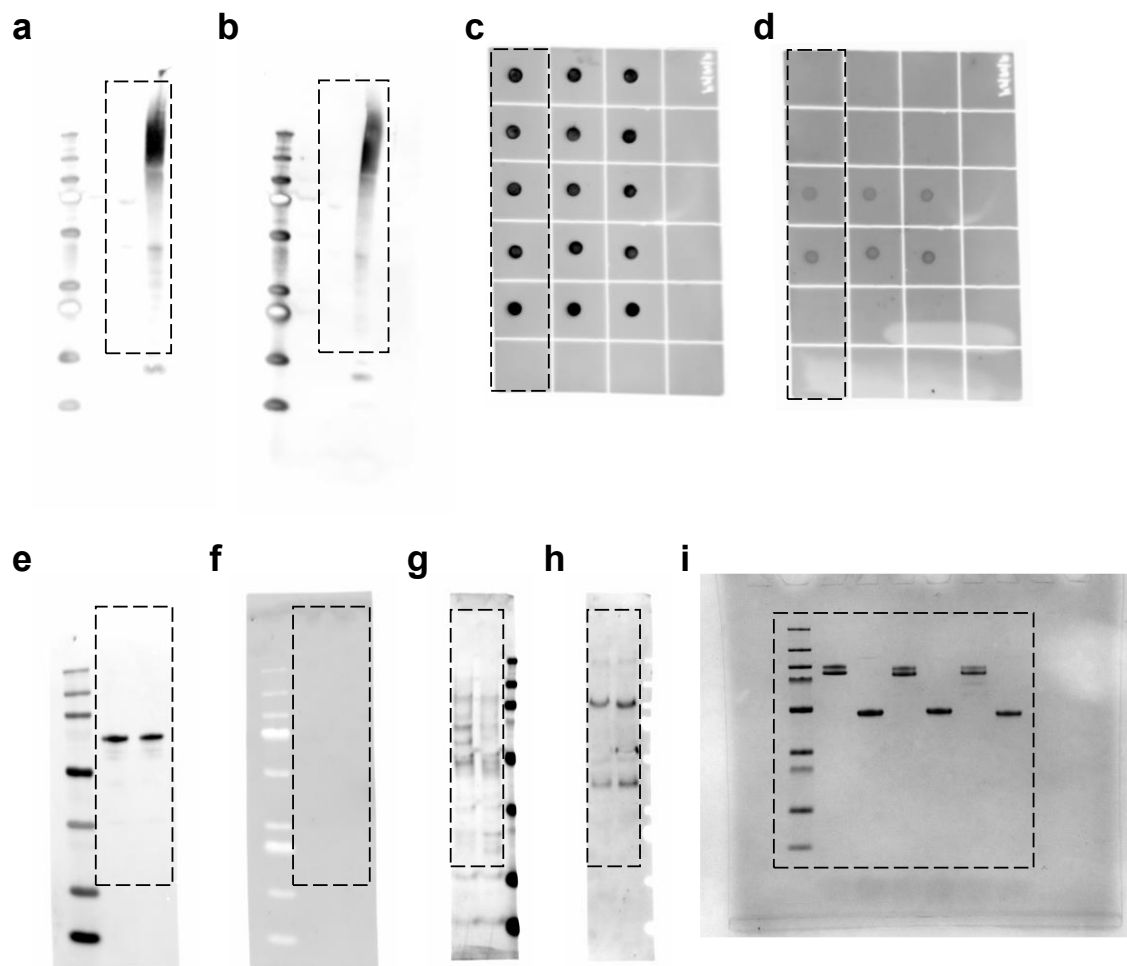
Supplementary Figure 6. Characterization of tau aggregation was performed with bis-ANS fluorescence spectroscopy. **(a)** A control nanobody Fc fusion, **(b)** bivalent OT2.4-Fc, or **(c)** bivalent OT2.6-Fc was mixed with tau oligomers in a 2:1, 4:1, or 8:1 molar ratio. These mixtures or tau oligomer containing no nanobody were used to seed tau monomer (1:100 seed:monomer). After incubation for 48 hours, bis-ANS fluorescence intensity was used to quantify tau aggregation.¹ This experiment was performed in triplicate, and error bars indicate standard deviation. **** $P < 0.0001$, *** $P < 0.001$, ** $P < 0.01$, * $P < 0.05$, ns: not significant, determined by two-way ANOVA.



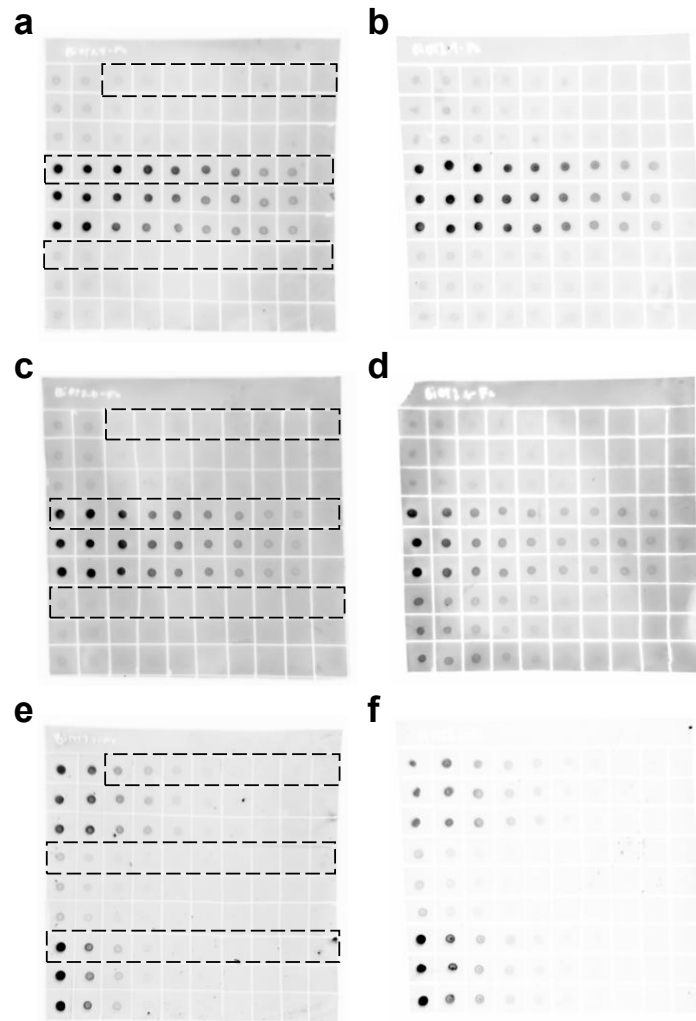
Supplementary Figure 7. Lysates of human brain tissue samples from five patients with AD and five controls were run on western blots, and binding with tau oligomer-specific antibody T22 was evaluated. This membrane was also stained with bivalent OT2.6-Fc (**Figure 6b**) and AT8 (**Figure 6d**). Ponceau S staining of this membrane is shown in **Supplementary Figure 8d**, and an unprocessed image of this membrane is shown in **Supplementary Figure 11g**. An unprocessed image of GAPDH staining is shown in **Supplementary Figure 11f**.



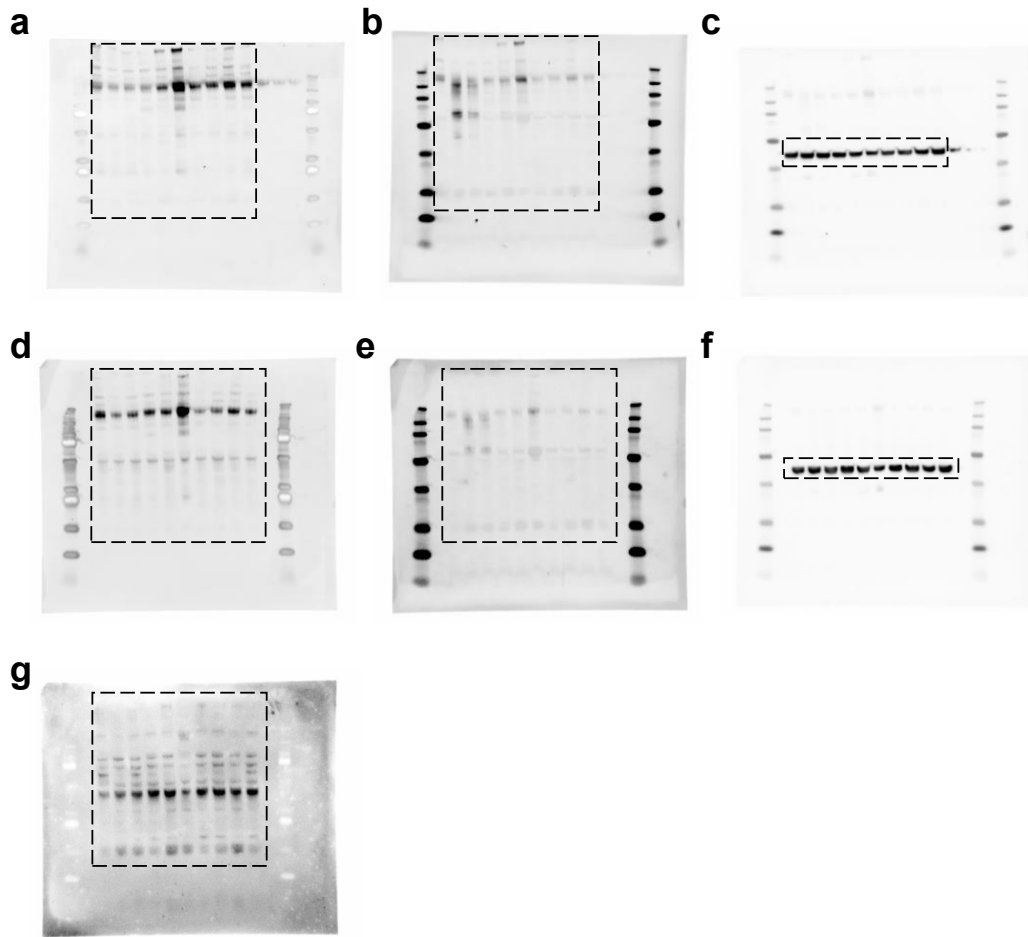
Supplementary Figure 8. Ponceau staining of western blots from **(a)** Figure 3a, **(b)** Figure 3b, **(c)** Figures 6a and c, **(d)** Figures 6b and d and Supplementary Figure 7, **(e)** Supplementary Figure 3c and d, and **(f)** Supplementary Figure 3e and f.



Supplementary Figure 9. Unprocessed images of immunoblots from (a) Figure 3a, (b) Figure 3b, (c) Supplementary Figure 3a, (d) Supplementary Figure 3b, (e) Supplementary Figure 3c, (f) Supplementary Figure 3d, (g) Supplementary Figure 3e, (h) Supplementary Figure 3f, and (i) Supplementary Figure 4.



Supplementary Figure 10. Independent repeats of dot blots used to assess tau oligomer specificity of nanobodies **(a-b)** OT2.4, **(c-d)** OT2.6, and **(e-f)** MT3.1. These images are also unprocessed images of dot blots from Figure 4a with **(a)** bivalent OT2.4-Fc staining, **(c)** bivalent OT2.4-Fc staining, and **(e)** bivalent MT3.1-Fc staining.



Supplementary Figure 11. Unprocessed images of western blots from **(a)** Figure 6a, **(b)** Figure 6c, **(c)** Figure 6a and c, **(d)** Figure 6b, **(e)** Figure 6d, **(f)** Figure 6b and d and Supplementary Figure 7, and **(g)** Supplementary Figure 7.

	Specificity	Binding Site	Format	Reference
OT2.4	oligomer	conformational, 133-147, 177-195, 343-367, 413-427	nanobody	
OT2.6	oligomer	conformational, 121-139, 149-163, 209-223, 373-391	nanobody	
TOC1	dimer, oligomer	conformational, 209-224	IgG	3,4
M204-scFv	oligomer	conformational, 275-280, 305-310	scFv	5
APNmAb005	oligomer	conformational	IgG	6
TOMA1	oligomer	conformational	IgG	7,8
2C5	oligomer, fibril		nanobody	9
TNT1	aggregates, pretangles	conformational, 7-12	IgG	10
TNT2	aggregates, pretangles	conformational, 7-12	IgG	10
2B8	pretangles, tangles	271-295, 307-331	nanobody	11
VDW	monomer, fibril	305-317	nanobody	12
MC1	fibril	conformational, 7-9, 313-322	IgG	13
ATA1.459.3	fibril	conformational, 16-20	scFv	14
WA2.22	fibril	conformational	nanobody	15
MT3.1	monomer, oligomer, fibril	125-130, 275-280, 306-311, 390-395	nanobody	16
Tau13	monomer, oligomer, fibril	9-18	IgG	17
Tau5	monomer, oligomer, fibril	218-225	IgG	18
VHH Z70		306-311	nanobody	19
VHH F8-2		373-378	nanobody	20
AT8	pTau	pS202, pT205	IgG	21
AT100	pTau	pT212, pS214	IgG	22

Supplementary Table 1. Tau-targeting monoclonal antibodies and antibody fragments.

Nanobody	Sequence
1 (OT2.6)	QVQLVESGGGLVQAGGSLRLSCAASGRTRFRYNAMGWYRQAPGKERELVAAITV RTGSTYYADSVKGRFTISRDNKNTVYVYLQMNSLKPEDTAVYYCAVDRDYLVRV SQLYREYGYWGQGTQVTVSS
2	QVQLVESGGGLVQAGGSLRLSCAASGITFRSYAMGWYRQAPGKEREFVAAITS GGASTYYADSVKGRFTISRDNKNTVYVYLQMNSLKPEDTAVYYCAARRPYKPYD YWGQGTQVTVSS
3	QVQLVESGGGLVQAGGSLRLSCAASGRTFYRYTMGWYRQAPGKERELVAAISF RAGRYYADSVKGRFTISRDNKNTVYVYLQMNSLKPEDTAVYYCAADQYLSAD YDYWGQGTQVTVSS
4	QVQLVESGGGLVQAGGSLRLSCAASGSIFRANAMGWYRQAPGKERELVAAITT GSRTYYADSVKGRFTISRDNKNTVYVYLQMNSLKPEDTAVYYCARRALYLPQRIN YSDAMDYWGQGTQVTVSS
5	QVQLVESGGGLVQAGGSLRLSCAASGYTFGRNTMGWYRQAPGKEREFVAAIT QSGGNTYYADSVKGRFTISRDNKNTVYVYLQMNSLKPEDTAVYYCNARLRPPYG WKYGYWGQGTQVTVSS
6	QVQLVESGGGLVQAGGSLRLSCAASGFTFGGANVMGWYRQAPGKERELVAAIT YGGGSTYYADSVKGRFTISRDNKNTVYVYLQMNSLKPEDTAVYYCAARSYRYW TQILYDYWGQGTQVTVSS
7	QVQLVESGGGLVQAGGSLRLSCAASGRFTFTSYTMGWYRQAPGKERELVAAITD RGGRTYYADSVKGRFTISRDNKNTVYVYLQMNSLKPEDTAVYYCNTVWGYHGG DEVDPHWGQGTQVTVSS
8	QVQLVESGGGLVQAGGSLRLSCAASGRTFVWNAMGWYRQAPGKERELVAAIT YRGASTYYADSVKGRFTISRDNKNTVYVYLQMNSLKPEDTAVYYCNARKYVTL KYDYWGQGTQVTVSS
9	QVQLVESGGGLVQAGGSLRLSCAASGRTFGRNAMGWYRQAPGKERELVAAITT GGSTNYADSVKGRFTISRDNKNTVYVYLQMNSLKPEDTAVYYCAATRWRKWYY YWGQGTQVTVSS
10 (OT2.4)	QVQLVESGGGLVQAGGSLRLSCAASGIISNNNAMGWYRQAPGKEREFVAAISTS GGSTYYADSVKGRFTISRDNKNTVYVYLQMNSLKPEDTAVYYCNRRVVERYWR GYWYREDGYWGQGTQVTVSS

Supplementary Table 2. Selected nanobody sequences.

Subject #	Primary Neuropathologic Diagnosis	Other Neuropathologic Diagnosis - Tau	Frontal NFT	Braak Stage	ABC	CERAD	Age at Death (yrs)	PMI (h)	Race	Sex
1	AD		frequent	VI	3	3	87	13	w	f
2	AD		frequent	VI	3	3	77	6.5	w	m
3	AD		frequent	VI	3	3	82	22.5	w	m
4	AD		frequent	VI	3	3	87	5	w	m
5	AD		frequent	VI	3	3	82	4.5	w	f
6	Control	PART	0	II	0	0	78	11.5	w	f
7	Control	PART	0	II	0	0	>89	5.5	w	m
8	Control	PART	0	III	1	1	>89	6	w	f
9	Control	PART	0	I	1	0	70	2.5	b	m
10	Control	PART	0	I	0	0	72	7	w	m

Supplementary Table 3. Sample data. PART = primary age-related tauopathy, ABC = Activities of Daily Living, Behavioral and Psychological Symptoms of Dementia, and Cognitive Function Dementia Scale, CERAD = Consortium to Establish a Registry for Alzheimer's Disease score.

References

- (1) Sengupta, U.; Carretero-Murillo, M.; Kaye, R. Preparation and Characterization of Tau Oligomer Strains. In *Methods in Molecular Biology*; Humana Press Inc., 2018; Vol. 1779, pp 113–146. https://doi.org/10.1007/978-1-4939-7816-8_9.
- (2) Lasagna-Reeves, C. A.; Castillo-Carranza, D. L.; Guerrero-Muñoz, M. J.; Jackson, G. R.; Kaye, R. Preparation and Characterization of Neurotoxic Tau Oligomers. *Biochemistry* **2010**, *49* (47), 10039–10041. <https://doi.org/10.1021/bi1016233>.
- (3) Ward, S. M.; Himmelstein, D. S.; Lancia, J. K.; Fu, Y.; Patterson, K. R.; Binder, L. I. TOC1: Characterization of a Selective Oligomeric Tau Antibody. *J Alzheimers Dis* **2013**, *37* (3), 593. <https://doi.org/10.3233/JAD-131235>.
- (4) Patterson, K. R.; Remmers, C.; Fu, Y.; Brooker, S.; Kanaan, N. M.; Vana, L.; Ward, S.; Reyes, J. F.; Philibert, K.; Glucksman, M. J.; Binder, L. I. Characterization of Prefibrillar Tau Oligomers in Vitro and in Alzheimer Disease. *Journal of Biological Chemistry* **2011**, *286* (26), 23063–23076. <https://doi.org/10.1074/jbc.M111.237974>.
- (5) Abskharon, R.; Seidler, P. M.; Sawaya, M. R.; Cascio, D.; Yang, T. P.; Philipp, S.; Williams, C. K.; Newell, K. L.; Ghetti, B.; DeTure, M. A.; Dickson, D. W.; Vinters, H. V.; Felgner, P. L.; Nakajima, R.; Glabe, C. G.; Eisenberg, D. S. Crystal Structure of a Conformational Antibody That Binds Tau Oligomers and Inhibits Pathological Seeding by Extracts from Donors with Alzheimer's Disease. *J Biol Chem* **2020**, *295* (31), 10662. <https://doi.org/10.1074/JBC.RA120.013638>.
- (6) Tai, H.-C.; Ma, H.-T.; Huang, S.-C.; Wu, M.-F.; Wu, C.-L.; Lai, Y.-T.; Li, Z.-L.; Margolin, R.; Intorcica, A. J.; Serrano, G. E.; Beach, T. G.; Nallani, M.; Navia, B.; Jang, M.-K.; Tai, C.-Y. The Tau Oligomer Antibody APNmAb005 Detects Early-Stage Pathological Tau Enriched at Synapses and Rescues Neuronal Loss in Long-Term Treatments. <https://doi.org/10.1101/2022.06.24.497452>.
- (7) Castillo-Carranza, D. L.; Sengupta, U.; Guerrero-Muñoz, M. J.; Lasagna-Reeves, C. A.; Gerson, J. E.; Singh, G.; Estes, D. M.; Barrett, A. D. T.; Dineley, K. T.; Jackson, G. R.; Kaye, R. Passive Immunization with Tau Oligomer Monoclonal Antibody Reverses Tauopathy Phenotypes without Affecting Hyperphosphorylated Neurofibrillary Tangles. *The Journal of Neuroscience* **2014**, *34* (12), 4260. <https://doi.org/10.1523/JNEUROSCI.3192-13.2014>.
- (8) Castillo-Carranza, D. L.; Gerson, J. E.; Sengupta, U.; Guerrero-Muñoz, M. J.; Lasagna-Reeves, C. A.; Kaye, R. Specific Targeting of Tau Oligomers in Htau Mice Prevents Cognitive Impairment and Tau Toxicity Following Injection with Brain-Derived Tau Oligomeric Seeds. *J Alzheimers Dis* **2014**, *40 Suppl 1* (S1). <https://doi.org/10.3233/JAD-132477>.
- (9) De Leiris, N.; Perret, P.; Lombardi, C.; Gözel, B.; Chierici, S.; Millet, P.; Debiossat, M.; Bacot, S.; Tournier, B. B.; Chames, P.; Lenormand, J. L.; Ghezzi, C.; Fagret, D.; Moulin, M. A Single-Domain Antibody for the Detection of Pathological Tau Protein in the Early Stages of Oligomerization. *J Transl Med* **2024**, *22* (1), 1–14. <https://doi.org/10.1186/S12967-024-04987-1>.
- (10) Combs, B.; Hamel, C.; Kanaan, N. M. Pathological Conformations Involving the Amino Terminus of Tau Occur Early in Alzheimer's Disease and Are Differentially Detected by Monoclonal Antibodies. *Neurobiol Dis* **2016**, *94*, 18–31. <https://doi.org/10.1016/J.NBD.2016.05.016>.
- (11) Jiang, Y.; Lin, Y.; Krishnaswamy, S.; Pan, R.; Wu, Q.; Sandusky-Beltran, L. A.; Liu, M.; Kuo, M. H.; Kong, X. P.; Congdon, E. E.; Sigurdsson, E. M. Single-Domain Antibody-Based Noninvasive in

Vivo Imaging of α -Synuclein or Tau Pathology. *Sci Adv* **2023**, *9* (19). <https://doi.org/10.1126/SCIADV.ADF3775>.

- (12) Abskharon, R.; Pan, H.; Sawaya, M. R.; Seidler, P. M.; Olivares, E. J.; Chen, Y.; Murray, K. A.; Zhang, J.; Lantz, C.; Bentzel, M.; Boyer, D. R.; Cascio, D.; Nguyen, B. A.; Hou, K.; Cheng, X.; Pardon, E.; Williams, C. K.; Nana, A. L.; Vinters, H. V.; Spina, S.; Grinberg, L. T.; Seeley, W. W.; Steyaert, J.; Glabe, C. G.; Ogorzalek Loo, R. R.; Loo, J. A.; Eisenberg, D. S. Structure-Based Design of Nanobodies That Inhibit Seeding of Alzheimer's Patient-Extracted Tau Fibrils. *Proc Natl Acad Sci U S A* **2023**, *120* (41). <https://doi.org/10.1073/pnas.2300258120>.
- (13) Jicha, G. A.; Bowser, R.; Kazam, I. G.; Davies, P. Alz-50 and MC-1, a New Monoclonal Antibody Raised to Paired Helical Filaments, Recognize Conformational Epitopes on Recombinant Tau. *J. Neurosci. Res* **1997**, *48*, 128–132. [https://doi.org/10.1002/\(SICI\)1097-4547\(19970415\)48:2<128::AID-JNR5>3.0.CO;2-E](https://doi.org/10.1002/(SICI)1097-4547(19970415)48:2<128::AID-JNR5>3.0.CO;2-E).
- (14) Desai, A. A.; Zupancic, J. M.; Trzeciakiewicz, H.; Gerson, J. E.; DuBois, K. N.; Skinner, M. E.; Sharkey, L. M.; McArthur, N.; Ferris, S. P.; Bhatt, N. N.; Makowski, E. K.; Smith, M. D.; Chen, H.; Huang, J.; Jerez, C.; Kane, R. S.; Kanaan, N. M.; Paulson, H. L.; Tessier, P. M. Flow Cytometric Isolation of Drug-like Conformational Antibodies Specific for Amyloid Fibrils. *bioRxiv* **2023**, 2023.07.04.547698. <https://doi.org/10.1101/2023.07.04.547698>.
- (15) Zupancic, J. M.; Smith, M. D.; Trzeciakiewicz, H.; Skinner, M. E.; Ferris, S. P.; Makowski, E. K.; Lucas, M. J.; McArthur, N.; Kane, R. S.; Paulson, H. L.; Tessier, P. M. Quantitative Flow Cytometric Selection of Tau Conformational Nanobodies Specific for Pathological Aggregates. *Front Immunol* **2023**, *14*, 1164080. <https://doi.org/10.3389/FIMMU.2023.1164080>.
- (16) McArthur, N.; Kang, B.; Rivera Moctezuma, F. G.; Shaikh, A. T.; Loeffler, K.; Bhatt, N. N.; Kidd, M.; Zupancic, J. M.; Desai, A. A.; Djeddar, N.; Bryksin, A.; Tessier, P. M.; Kayed, R.; Wood, L. B.; Kane, R. S. Development of a Pan-Tau Multivalent Nanobody That Binds Tau Aggregation Motifs and Recognizes Pathological Tau Aggregates. *Biotechnol Prog* **2024**, e3463. <https://doi.org/10.1002/BTPR.3463>.
- (17) García-Sierra, F.; Ghoshal, N.; Quinn, B.; Berry, R. W.; Binder, L. I. Conformational Changes and Truncation of Tau Protein during Tangle Evolution in Alzheimer's Disease. *Journal of Alzheimer's Disease* **2003**, *5* (2), 65–77. <https://doi.org/10.3233/JAD-2003-5201>.
- (18) Porzig, R.; Singer, D.; Hoffmann, R. Epitope Mapping of MAbs AT8 and Tau5 Directed against Hyperphosphorylated Regions of the Human Tau Protein. *Biochem Biophys Res Commun* **2007**, *358* (2), 644–649. <https://doi.org/10.1016/J.BBRC.2007.04.187>.
- (19) Danis, C.; Dupré, E.; Zejneli, O.; Caillierez, R.; Arrial, A.; Bégard, S.; Mortelecque, J.; Eddarkaoui, S.; Loyens, A.; Cantrelle, F.-X.; Hanouille, X.; Rain, J.-C.; Colin, M.; Buée, L.; Landrieu, I. Inhibition of Tau Seeding by Targeting Tau Nucleation Core within Neurons with a Single Domain Antibody Fragment. **2022**. <https://doi.org/10.1016/j.ymthe.2022.01.009>.
- (20) Dupré, E.; Clément, D. †; Danis, C.; Arrial, A.; Hanouille, X.; Homa, M. M.; Cantrelle, F. O.-X.; Merzougui, H.; Colin, M.; Rain, J.-C.; Buée, L.; Landrieu, I. Single Domain Antibody Fragments as New Tools for the Detection of Neuronal Tau Protein in Cells and in Mice Studies. **2019**. <https://doi.org/10.1021/acscemneuro.9b00217>.

- (21) Goedert, M.; Jakes, R.; Vanmechelen, E. Monoclonal Antibody AT8 Recognises Tau Protein Phosphorylated at Both Serine 202 and Threonine 205. *Neurosci Lett* **1995**, *189* (3), 167–170. [https://doi.org/10.1016/0304-3940\(95\)11484-E](https://doi.org/10.1016/0304-3940(95)11484-E).
- (22) Zheng-Fischhöfer, Q.; Biernat, J.; Mandelkow, E. M.; Illenberger, S.; Godemann, R.; Mandelkow, E. Sequential Phosphorylation of Tau by Glycogen Synthase Kinase-3beta and Protein Kinase A at Thr212 and Ser214 Generates the Alzheimer-Specific Epitope of Antibody AT100 and Requires a Paired-Helical-Filament-like Conformation. *Eur J Biochem* **1998**, *252* (3), 542–552. <https://doi.org/10.1046/J.1432-1327.1998.2520542.X>.